

Effect of Natural Gas Exsolution on Specific Storage in a Confined Aquifer Undergoing Water Level Decline

by Richard M. Yager¹ and John C. Fountain²

Abstract

The specific storage of a porous medium, a function of the compressibility of the aquifer material and the fluid within it, is essentially constant under normal hydrologic conditions. Gases dissolved in ground water can increase the effective specific storage of a confined aquifer, however, during water level declines. This causes a reduction in pore pressure that lowers the gas solubility and results in exsolution. The exsolved gas then displaces water from storage, and the specific storage increases because gas compressibility is typically much greater than that of water or aquifer material.

This work describes the effective specific storage of a confined aquifer exsolving dissolved gas as a function of hydraulic head and the dimensionless Henry's law constant for the gas. This relation is applied in a transient simulation of ground water discharge from a confined aquifer system to a collapsed salt mine in the Genesee Valley in western New York. Results indicate that exsolution of gas significantly increased the effective specific storage in the aquifer system, thereby decreasing the water level drawdown.

Introduction

Specific storage S_s of a confined aquifer is defined as the volume of water released from storage in a unit volume of aquifer material, under a unit decline in hydraulic head (Bear 1979). Specific storage is related to the compressibility of the aquifer material and fluid by the following relation:

$$S_s = \rho g (\alpha + n\beta) \quad (1)$$

where ρg is specific weight of water [$\text{ML}^{-2}\text{T}^{-2}$], α is compressibility of aquifer material [$\text{ML}^{-1}\text{T}^{-2}$]⁻¹, β is fluid compressibility [$\text{ML}^{-1}\text{T}^{-2}$]⁻¹, and n is porosity [dimensionless].

Specific storage generally is treated as a constant in ground water flow analyses, but variations in S_s can occur where aquifer compressibility changes as a result of inelastic compaction and permanent rearrangement of the grains that form the aquifer (Leake 1991).

Estimates of S_s for unconsolidated aquifer material generally range from 3×10^{-6} to 1×10^{-5} m⁻¹ (Riley 1998). Heywood (1998) computed S_s values ranging from 7.9×10^{-6} to 1.1×10^{-5} m⁻¹ for Rio Grande alluvium in Texas using the method of Riley (1969) relating changes in fluid pressure to aquifer compression determined from extensometer measurements. Analysis of earth tide strains in the same sediments using the method of Bredehoeft (1967) yielded S_s values of 3.6×10^{-6} to 5.6×10^{-5} m⁻¹. Nelson (1982) also used extensometer measurements to estimate an S_s

value of 7.6×10^{-6} m⁻¹ for glacial drift near Anchorage, Alaska. For an incompressible aquifer matrix with a porosity of 0.3, the minimum value of specific storage is about 1.3×10^{-7} m⁻¹.

Relation of Gas Solubility to Specific Storage

Specific storage of a confined aquifer undergoing a water level decline accounts for the amount of water released from storage in response to: (1) aquifer compression ($\rho g \alpha$) through increasing effective stress σ_e ; and (2) expansion of water ($\rho g n \beta$) through decreasing fluid pressure p . Decreasing fluid pressure in aquifers that contain dissolved gas also lowers the gas solubility, allowing gas to exsolve from the water as a free phase if the dissolved-gas concentration exceeds the solubility limit and if capillary effects can be overcome. Gas exsolution can significantly increase the effective specific-storage of the aquifer because the exsolved gas replaces water in the pore space, allowing additional releases from storage, and gas compressibility is about 100 times greater than aquifer compressibility under pressures commonly observed in shallow confined aquifers (less than 1.5 MPa). These effects can be accounted for in simulations of ground water flow through a gas-partitioning equation that relates the volume of gas exsolved to the decline in hydraulic head. Gas solubility is explicitly included in many petroleum-reservoir simulators; however, only the solubility of natural gas in the oil phase is considered and the solubility of gas in the water phase is generally omitted (Wang et al. 1996).

The gas-partitioning equation can be derived from the equation of mass for gas in an arbitrary volume of aquifer material V_a undergoing pressure decline, namely,

$$M = C_w V_w + C_v V_v + C_w V_v \quad (2)$$

where M is initial mass of gas prior to pressure decline [M], C_w is concentration of gas in water [ML^{-3}], V_w is volume of water

¹U.S. Geological Survey, 30 Brown Rd., Ithaca, NY 14850; ryager@usgs.gov

²Department of Geology, State University of New York-Buffalo, Box 603050, Buffalo, NY 14260-3050; fountain@ascu.buffalo.edu

Received March 2000, accepted January 2001.

[L³], C_v is concentration of gas in the vapor phase [ML⁻³], and V_v is volume of vapor [L³].

The third term on the right-hand side of Equation 2 represents the gas dissolved in water released from storage as a result of the pressure decline. The sum of the water- and vapor-filled volumes equals the volume of pore space.

$$V_w + V_v = nV_a \quad (3)$$

Combining Equations 2 and 3, and solving for V_v, gives the gas-partitioning equation

$$V_v = \frac{M - C_w n V_a}{C_v} \quad (4)$$

For gases that follow Henry's law, C_w is related to the gas concentration in the vapor phase C_v by the dimensionless Henry's law constant K_h:

$$C_w = K_h C_v \quad (5)$$

The concentration of gas in water C_w at absolute pressure p is also related to the gas solubility C₀ measured at a reference pressure p₀:

$$C_w = C_0 \frac{p}{p_0} \quad (6)$$

If the pore space was initially saturated with water (V_w = nV_a), and the water was saturated with gas, then M = C_wV_w at the bubble pressure p_b that prevailed before the water level decline, and

$$M = C_0 \frac{p_b}{p_0} n V_a \quad (7)$$

Combining Equations 5, 6, and 7 with Equation 4 and simplifying gives

$$V_v = \frac{(p_b - p)nV_a}{pK_h} \quad (8)$$

An equation similar to Equation 8 was recently presented by Jarsjo and Destouni (2000, Equation 3) to compute the volume of gas exsolved near boreholes in response to drawdown induced by hydraulic tests.

Hydraulic head h is defined in terms of gauge pressure p_{gauge}:

$$h = \frac{p_{gauge}}{\gamma} + z \quad (9)$$

where γ is the specific weight of water [ML⁻²T⁻²], and z is elevation [L].

Gauge pressure is defined as absolute pressure minus atmospheric pressure p_{atm}

$$p_{gauge} = p - p_{atm} \quad (10)$$

Expressing pressure in terms of head results in the following equation:

$$p = (h - z)\gamma + p_{atm} \quad (11)$$

Substituting this equation for pressure into Equation 8 and simplifying gives

$$V_v = \frac{(h_b - h)nV_a}{(h - z + h_{atm})K_h} \quad (12)$$

where h_b is head corresponding to gas saturation [L], z is elevation of the midpoint of the aquifer [L], and h_{atm} = p_{atm}/γ.

The specific storage resulting from gas exsolution S_{sg} is the volume V_v of gas produced (water released) from a unit volume of aquifer material V_a under a unit change in head (h_b - h = 1) or

$$S_{sg} = \frac{n}{(h - z + h_{atm})K_h} \quad (13)$$

The effective specific storage S_s' can be computed as the sum of S_s (Equation 1) and S_{sg} (Equation 13) to yield

$$S_s' = S_s + S_{sg} \quad (14)$$

Equations 13 and 14 indicate that the effective specific storage of a confined aquifer containing dissolved gas and undergoing water level decline is not constant, but is a function of head (pressure), which varies temporally and spatially. Increasing fluid pressure during water level recovery would result in solution of the released gas and decreased specific storage values as the volume of free gas in the pore volume declined.

The derived relation between gas solubility and effective specific storage (Equation 13) overestimates the contribution of gas exsolution to specific storage because it assumes that all of the exsolved gas remains within the aquifer and is not lost through ground water withdrawal or migration. However, accounting for these effects would require simulation of gas transport, and other sources of uncertainty, such as the initial gas concentration in the aquifer, probably represent greater sources of error in the calculated volume of exsolved gas. The relation also neglects the partial pressure of water vapor, which is generally small relative to the total pressure. For example, the partial pressure of water at 10°C is only 1.1 kPa, or 0.5% of the total pressure of 150 kPa at a 15 m depth.

Water Level Decline in a Confined Aquifer

A collapse of the bedrock ceiling in parts of a salt mine in western New York (Figure 1) in March and April 1994 allowed water from overlying aquifers to flood the mine. A three-dimensional ground water flow model was developed to simulate the response of the aquifer system to mine flooding. Model simulations were used to estimate the time required for water levels in the aquifer to return to pre-collapse conditions and the extent of land subsidence caused by compression of fine-grained sediments (Yager et al. 2001).

Hydrogeology

The glacial-drift aquifer system within the Genesee Valley consists of three aquifers separated by two confining layers in a bedrock valley (Figure 2a). The uppermost (unconfined) aquifer consists of alluvial sediments 6 to 18 m thick, a middle confined

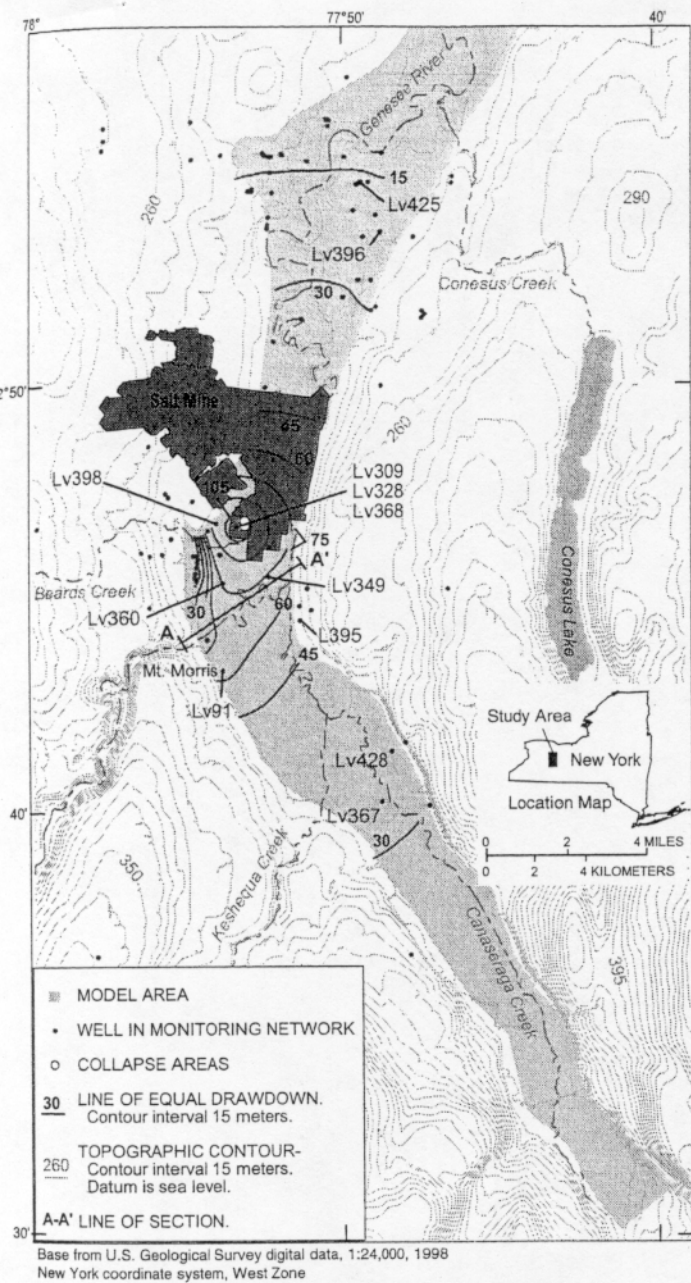


Figure 1. Location and extent of mined area, Livingston County, New York, site of 1994 mine collapse, and distribution of drawdown in lower aquifer in January 1996 in response to mine flooding.

aquifer consists of glaciofluvial sand and gravel 3 to 5 m thick, and a lower aquifer consists of glaciofluvial sand and gravel about 7.5 m thick overlying the bedrock valley floor. The upper and middle aquifers are separated by an upper confining layer of lacustrine sediments and till as much as 75 m thick, and the middle and lower aquifers are separated by a lower confining layer of undifferentiated glaciolacustrine sediments as much as 75 m thick. The principal permeable zones in the bedrock consist of fractures near the contact between two carbonates—the Devonian Onondaga Limestone and the Silurian Bertie Limestone (Figure 2a). The unconsolidated glacial-drift aquifers are hydraulically connected at the edges of the confining layers, and permeable zones in the bedrock subcrop beneath the north end of the valley.

Ground water within the valley originates as precipitation on the valley floor and the surrounding uplands and discharges to stream channels or as underflow to downgradient areas. Recharge enters the deep confined aquifers along the sides of the valley,

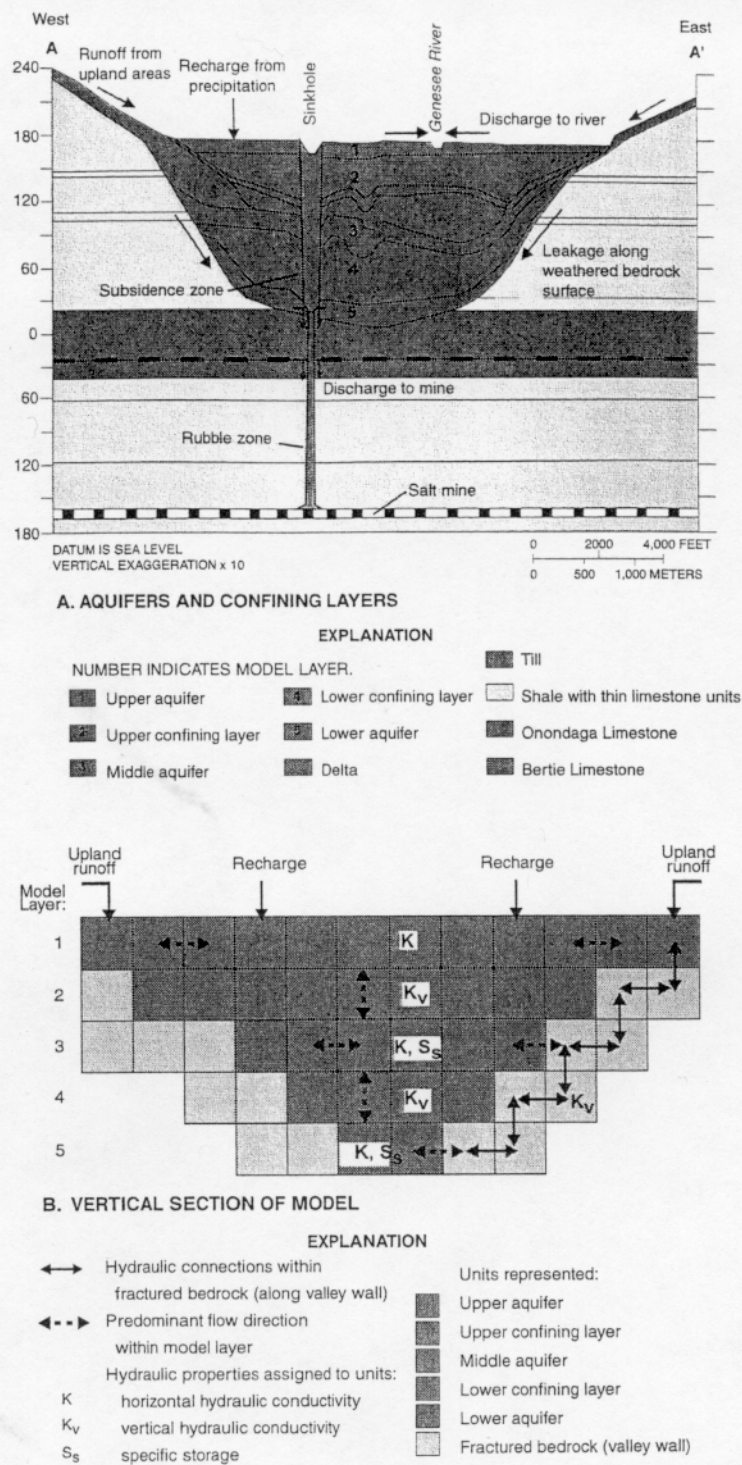


Figure 2. Generalized sections in the Genesee Valley: (a) aquifers and confining layers; (b) representation of aquifer system in three-dimensional flow model (line of section shown in Figure 1).

particularly in the southern part, where permeable morainal and deltaic deposits connect the upper aquifer with the deeper middle and lower aquifers. The hydraulic-head distribution in the deeper aquifers under precollapse conditions is assumed similar to that of the upper (unconfined) aquifer.

Effects of Mine Collapse

A salt layer in the shales beneath the Onondaga and Bertie limestones has been mined since 1885. In March and April 1994, parts of the salt mine catastrophically collapsed, allowing ground water from overlying aquifers to flood the mine and causing rapid draw-

downs throughout the aquifer system. Mining was halted in September 1995, and the mine shafts were sealed after the mine became completely flooded in January 1996.

The collapses allowed water from the lower aquifer to drain through a rubble zone into the mine. The drainpoint is at an altitude of 12 m above sea level (Figure 2a), which is 150 m lower than the aquifer's natural outlet at the north end of the Genesee Valley. This drainage altered the hydraulic gradients in the deeper aquifers and reversed the direction of flow north of the collapse area. Water levels in the lower aquifer had dropped as much as 120 m by January 1996, when the mine was completely flooded, and several domestic wells screened in the middle aquifer went dry. Drawdowns of 15 to 40 m were recorded at wells 12 km north and south of the collapse area (Figure 1). Water levels in upland areas and in most of the upper aquifer were apparently unaffected by the collapse, although drawdowns of 2 m in the upper aquifer could have occurred near the collapse area. Water levels in the collapse area had recovered 90 m (75%) about two years after drainage to the mine had ceased.

Methane and hydrogen sulfide were detected in the salt mine after the collapses and accumulated to unsafe levels periodically through the summer of 1994. Several bedrock wells, originally drilled in the collapse area as part of a grouting program undertaken to save the mine, were used to vent the gas, and three of the wells were flared in May 1995. Some water wells screened in the aquifer system as far as 10 km from the collapse area began to produce gas after the collapse. Gas was flared from two wells screened in the middle aquifer near the bedrock surface—Lv398 on the west side of the valley and Lv428 on the east side of the valley (Figure 1), after the wells went dry in April and July 1994, respectively. Gas was also produced in two wells screened in the lower aquifer—Lv91 in Mt. Morris (December 1994) and Lv368 in the collapse area (October 1995). Gas production ceased in the fall of 1998 in well Lv398 but continues (1999) in well Lv428 and supplies heating fuel to three homes. Releases of biogenic gas (methane) from several wells affected by water level declines suggest that exsolved gas was present as a free phase over a wide area during mine flooding.

Dissolved Gases in Ground Water

Natural gas is commonly encountered during drilling in the middle and lower aquifers in the Genesee Valley (Hall, oral communication 1996), and methane and hydrogen sulfide were reported during the sampling of several wells screened in these aquifers in 1966 (Kammerer and Hobba, 1967). Methane is a common component of ground water, typically as a dissolved phase at concentrations less than 10 mg/L (Barker and Fritz 1981; Whiticar et al. 1986). Methane is of two primary types: biogenic methane, produced by bacterial decay of organic matter, and thermogenic methane, produced during thermal generation of petroleum hydrocarbons. The local bedrocks in western New York are known to contain thermogenic gas (Jenden et al. 1993), but the concentrations of thermogenic methane in shallow ground water (less than 30 m depth) are typically low and accumulate to more than 10 mg/L only near local sources such as wells, pipelines, or fractures that tap a gas reservoir (Stahl et al. 1981; Jones and Drozd 1983; Faber and Stahl 1984). Biogenic methane, in contrast, has been found at or near saturation at shallow depths in many locations (King and Wiebe 1978; Whiticar et al. 1986; Adrian et al. 1994; Parkin and Simpkins 1995; Romanowicz et al. 1995; Martini et al. 1996).

Biogenic methane can be distinguished from thermogenic methane by the relative abundance of heavier hydrocarbons and

Table 1
Methane-to-Ethane Ratios of Gases Collected from Venting Wells in 1995 and from Ground Water Samples in 1999

Well	Aquifer	Ratio of Methane to Ethane	Methane Concentration mg/L
Gas sampled in 1995:			
Lv91	lower aquifer	135	—
Lv309	carbonate bedrock	12.7	—
Lv328	carbonate bedrock	21.0	—
Lv349	middle aquifer ^a	50.0	—
Lv395	middle aquifer	84.2	—
Lv398	middle aquifer	53.9	—
Lv428	middle aquifer	66.1	—
Water sampled in 1999:			
Lv360	lower aquifer	19.8	38
Lv367	lower aquifer	13.9	14
Lv368	lower aquifer	6.6	2

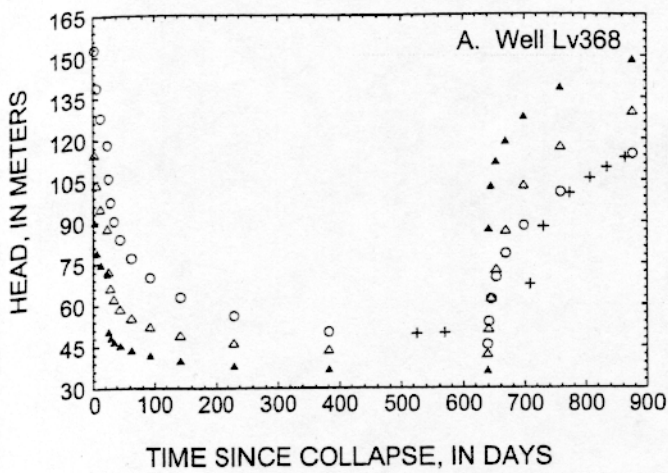
^aGas sampled during drilling.

lighter (more negative) isotopic composition of carbon (James 1983; Whiticar et al. 1986). Biogenic methane contains negligible amounts of ethane and heavier hydrocarbons and typically has $\delta^{13}\text{C}$ values less than -50‰ . In contrast, 14% to 21% of the hydrocarbons in thermogenic gas in the near-surface bedrocks in western New York are ethane, propane, and butane; the methane-to-ethane ratios are less than 20, and $\delta^{13}\text{C}$ values in methane range from -32‰ to -41‰ (Jenden et al. 1993). The solubility of methane at 1 atmosphere pressure is 24.4 mg/L (McAulliffe 1966) and increases with pressure following Henry's law to 863 mg/L at 3.4 MPa (~ 350 m of head) (Li and Ngheim 1986; Song et al. 1997).

Gas Sampling and Analysis

Gas exsolving from seven wells in the Genesee Valley was sampled in 1995 during mine flooding: four wells screened in the middle aquifer, one well screened in the lower aquifer and two bedrock wells (Figure 1). Gas also was collected from water samples in three wells screened in the lower aquifer in 1999 after the mine was completely flooded. Samples were collected from wells venting gas through tubing that connected a valve installed at the well head to a stainless-steel gas-sampling vessel or an aluminized mylar sampling bag (Milliken, written communication 1995). Water samples were collected with a stainless-steel sampler manufactured by Westbay Instruments under hydrostatic pressure. The Westbay sampler was evacuated with a hand pump to create a vacuum of 64 cm of mercury, and a valve in the sampler was opened from land surface to allow water to enter the sampler at a specified depth in the well. After retrieval, the sampler was connected to an evacuated Tedlar bag, and the valve on the sampler was opened. A combination of the expansion of headspace gas and an exsolution of dissolved gas, both resulting from the drop in pressure, caused gas to rapidly enter the bag.

Gases were analyzed by a gas chromatograph (GC) equipped with a flame-ionization detector through direct injection at 110°C onto a 2 m, 3.2 mm diameter stainless-steel Hayesep D column. The instrument was calibrated daily with 99% calibration gases diluted with nitrogen and standards run at least every 10 samples. Some gas samples also were analyzed with a Century OVA 128 GC that used a nonheated column and a flame-ionization detector. Many



EXPLANATION

- + Observed
- Model A (specific storage estimated by regression)
- ▲ Model A (specific storage fixed at $7.6 \times 10^{-6} \text{ m}^{-1}$)
- △ Model B (with gas exsolution)

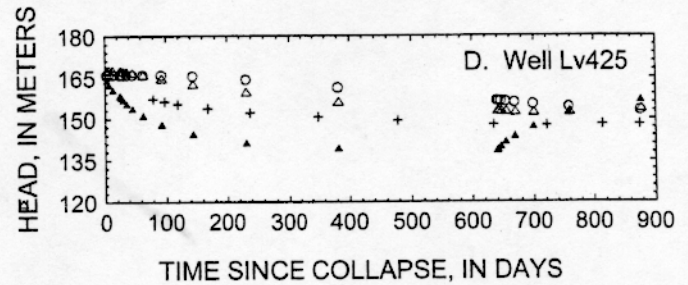
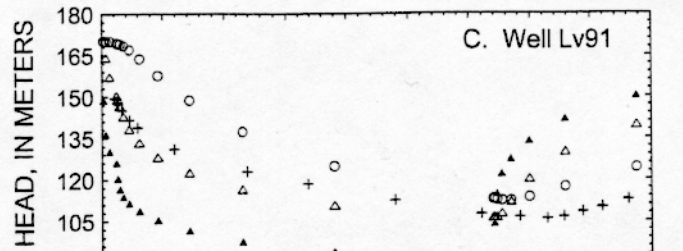
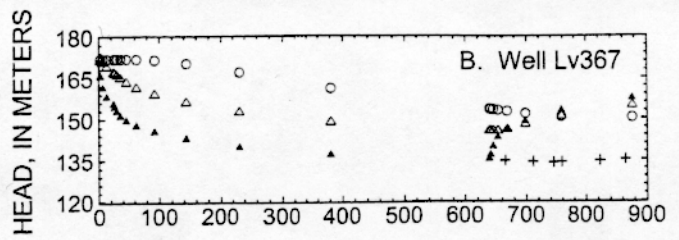


Figure 3. Water levels predicted by transient simulations with specific storage values specified from literature values, estimated by regression (model A), computed considering gas exsolution (model B), and measured in the lower aquifer: (a) near collapse area, well Lv368; (b) 11 km south of collapse, well Lv367; (c) 5 km south of collapse, near Mt. Morris, well Lv91; (d) 13 km north of collapse, well Lv425.

samples were diluted for this analysis because the calibration limit for the instrument was only 1000 mg/L; therefore, only methane-to-ethane ratios (not affected by the dilution) from these analyses were used.

Results

Gas from five of the seven wells sampled in 1995 had methane-to-ethane ratios ranging from 54 to 135, which indicate that the gas was primarily biogenic (Table 1). The relatively light isotopic composition of carbon ($\delta^{13}\text{C}$ value of -55.1‰) in the methane from well Lv395 is consistent with this finding. The biogenic gas probably exsolved from ground water as heads in the aquifer were lowered during the flooding of the mine, and the wide distribution of gas-producing wells suggests that gas exsolved over much of the confined aquifer system. In contrast, gas from wells near the collapse area (Lv309 and Lv328) had methane-to-ethane ratios ranging from 13 to 21, similar to those of thermogenic gas in western New York. The thermogenic gas in the collapse area probably entered both the lower aquifer and the mine from a fracture zone in the Bertie limestone where gas had previously been detected in other boreholes (Milliken, oral communication 1996).

Methane concentrations in water samples collected in 1999 ranged from 2 to 38 mg/L, much less than concentrations expected near saturation (320 to 420 mg/L). The methane-to-ethane ratios of 7 to 20 indicate that the gas was primarily thermogenic. The methane concentrations in the water samples suggest that the lower aquifer does not contain high levels of dissolved gas at present, probably as a result of exsolution and subsequent migration of gas during flooding of the mine. Measured concentrations only qualitatively

represent actual methane concentrations in ground water, however, because the sampled wells are open to the atmosphere, and some methane could be lost through diffusion through the water column in the well.

The source of the biogenic gas could be Devonian black shales that border the lower aquifer in the bedrock valley. Production of biogenic methane in shallow ground water can be limited by high concentrations of dissolved sulfate, but analyses of water sampled from the lower aquifer indicate sulfate concentrations are generally less than 20 mg/L (Yager et al. 2001). While no chemical analyses are available for redox species in the lower aquifer, the presence of hydrogen sulfide noted by drillers suggests a reduced geochemical environment consistent with a biogenic origin of dissolved methane.

Simulation of Ground Water Discharge and Gas Exsolution

Ground water flow within the aquifer system was simulated with MODFLOWP (Hill 1992), a three-dimensional flow model constructed to provide inverse estimates of parameters representing aquifer properties. Conditions before and after the mine collapse were simulated. Parameter values representing aquifer properties were adjusted through steady-state and transient-state simulations to produce a model that approximated ground water levels and flow rates measured prior to the mine collapse, during flooding of the mine, and during a period of water level recovery after the mine was filled. Hydraulic heads computed by steady-state simulations provided initial conditions for a 29-month transient-state simulation representing drainage from the aquifer system to the mine (March 1994 through December 1995) and recovery of water levels after the mine

Table 2
Optimum Parameter Values Estimated for Confined-Aquifer System in Model A (Constant Specific Storage),
Their Approximate 95% Confidence Intervals, and Values Estimated by Model B (With Gas Exsolution)

Variable	Model A	Approximate Individual Confidence Interval	Coefficient of Variation (%) ^a	Model B
Hydraulic conductivity, m/d				
middle aquifer	1.1	0.4 – 3.3	30%	1.8
lower aquifer	91	55 – 150	26%	73
Vertical hydraulic conductivity, m/d				
upper confining layer	3.3×10^{-5}	—	—	3.3×10^{-5b}
lower confining layer	3.7×10^{-4}	$1.3 \times 10^{-4} - 9.8 \times 10^{-4}$	4%	5.4×10^{-4}
collapse area (lower confining layer)	8.2×10^{-3}	$7 \times 10^{-5} - 0.94$	37%	7.8×10^{-3}
Specific storage, m ⁻¹				
upper confining layer	3.3×10^{-5b}	—	—	3.3×10^{-5b}
middle aquifer	2.3×10^{-4}	$4.3 \times 10^{-5} - 1.2 \times 10^{-3}$	5%	7.6×10^{-6}
lower confining layer	1.6×10^{-5b}	—	—	1.6×10^{-5b}
lower aquifer	9.5×10^{-4}	$4.6 \times 10^{-4} - 2 \times 10^{-3}$	3%	7.6×10^{-6}
Bubble press p_b , MPa				
middle aquifer	—	—	—	0.7
lower aquifer	—	—	—	1.6
Model error				
Sum of squared errors, m ²	3.75×10^4			4.8×10^4
Standard error in heads, m	10			11.3
Discharge to mine, L/s		Observed		
March 1994	570	310		323
September 1994	790	1300		478
^a Coefficient of variation on log-transformed parameter.				
^b Specified value in nonlinear regression.				

had completely filled (January 1996 through August 1996). Two alternative models were considered: model A, in which the specific storage was constant during the transient-state simulation, and model B, in which specific storage varied as a result of exsolution and subsequent solution of methane.

Model Design

The three aquifers and two confining layers within the unconsolidated glacial deposits were represented by five model layers (Figure 2b) and a uniformly spaced grid with a cell size of 91 m that represented 159 km² in the Genesee Valley. Recharge to the unconfined aquifer was represented by a constant-flow (Neumann) boundary with higher recharge rates specified along valley walls to account for additional recharge from upland runoff. Outflow through the northern (downgradient) boundary, and flow to and from perennial streams, was represented by head-dependent (Cauchy) boundaries; the contact between the aquifer system and the shale bedrock at the valley wall was represented by a no-flow boundary. Vertical leakage through permeable deposits and (or) bedrock fractures along the valley wall was represented by hydraulic connections between adjacent model layers (Figure 2b). In transient-state simulations, constant-head (Dirichlet) boundaries were specified at the two collapse sites in model layer five (lower aquifer) to represent drainage from the aquifer system to the mine from March 1994 through December 1995.

Constant Specific Storage (Model A)

Six parameters representing horizontal hydraulic conductivity and specific storage of model layers three and five (middle and lower

aquifers, respectively), and vertical hydraulic conductivity of model layer four (lower confining layer) were estimated through transient-state simulations based on 354 water level measurements recorded in 51 wells from March 1994 through August 1996, and two estimates of ground water discharge to the mine in March and September 1994 (Table 2). The distribution of drawdown in January 1996 computed by model A was similar to the measured distribution, and the standard error in heads was 10 m. Computed drawdowns near the collapse area (123 m) were overpredicted by less than 3 m, and the predicted change in drawdown with time was in close agreement with measured drawdowns at individual wells (Figure 3a). Drawdowns 11 km to the north (10 m) and 13 km to the south (15 m) were generally underpredicted by about 5 m and 18 m, respectively (Figure 3b and 3c).

Computed discharges to the mine in April 1994 (570 L/s) were 100% greater than the values estimated from the observed rate of mine flooding, and computed discharges to the mine in September 1994 (790 L/s) were 40% less than the values estimated. The computed water budget indicated that most of the water discharged to the mine was ground water released from storage (Table 3a), and that most of the inflow was from storage in the lower aquifer (58%). Storage from confining layers contributed only about 10% of the water (Table 3b), an estimate confirmed by one-dimensional simulations of flow in the confining layers calibrated to measurements of pore pressure and land subsidence (Yager et al. 2001). The estimated volume of water discharged to the mine (2.8×10^{10} L) was only 55% to 60% of the estimated mine volume because drawdowns south of the mine were underpredicted. This bias suggests that model A does not accurately represent significant processes that affect ground water flow.

Table 3
Simulated Water Budget for Aquifer System in Model A (Constant Specific Storage) During Period of Mine Flooding, March 1994 Through January 1996: (A) Entire Aquifer System (Model Layers 1 Through 5). (B) Confined Aquifer System (Model Layers 2 Through 5). [Flow Volumes are in Millions of Cubic Meters]

Inflow			Discharge		
Source	Volume	Percentage of Total	Location	Volume	Percentage of Total
A. Entire aquifer system (model layers 1 through 5)					
Storage	24	11	River and streams	181	84
Recharge and upland runoff	105	49	Underflow	5	3
River and streams	69	32	Salt mine	29	13
Underflow	17	8			
Total	215	100	Total	215	100
B. Confined part of aquifer system (model layers 2 through 5)					
Storage					
upper confining layer	0.2	< 1			
middle aquifer	1.9	6			
lower confining layer	2.7	9			
lower aquifer	17	58			
Underflow					
middle aquifer	0.6	2	Underflow		
lower aquifer	< .1	< 1	middle aquifer	< .1	< 1
			lower aquifer	0.7	3
Vertical leakage					
valley walls	5.9	19	Vertical leakage		
deltaic deposits	1.4	5	valley walls	0.2	< 1
			salt mine	29	97
Total	29.9	100	Total	29.9	100

Coefficients of variation of the log-transformed parameter values estimated by nonlinear regression indicated that model A was sensitive to the estimated parameters and that, if the values for these parameters were changed, model error would increase. Coefficients of variation for vertical hydraulic conductivity of the lower confining layer and specific storage of the middle and lower aquifers were less than 10%, indicating that the model was most sensitive to these three parameters (Table 2). Specific-storage values estimated for the middle and lower aquifers were $2.3 \times 10^{-4} \text{ m}^{-1}$ and $9.5 \times 10^{-4} \text{ m}^{-1}$, respectively, which is much larger than the range of values ($2.3 \times 10^{-6} \text{ m}^{-1}$ to $7 \times 10^{-6} \text{ m}^{-1}$) estimated for other sand and gravel aquifers from extensometer measurements of land subsidence. Assigning a lower value of specific storage ($7 \times 10^{-6} \text{ m}^{-1}$) greatly increased model error, however, and no combination of the remaining parameter values was found through nonlinear regression that provided an acceptable match to the measured water levels. The response of the confined aquifer system when simulated with the lower specific-storage value was more rapid than the observed response, particularly during the period of water level recovery after the mine was filled (Figure 3).

Gas Exsolution (Model B)

The effects of gas exsolution were incorporated into the computer program MODFLOWP by computing the effective specific storage S_s' for every time step of the transient-state simulation. The specific storage resulting from gas exsolution S_{sg} was calculated for each model cell through Equation 13 with heads obtained from the previous time step, a porosity n of 0.3 and a K_h -value for methane of 27.02 (Schwarzenbach et al. 1993). The effective specific storage S_s' (Equation 14) was then used to compute heads for the succeeding time step. Values of S_{sg} decreased as water levels recovered to represent solution of gas, under the assumptions that the gas was

trapped and did not escape from the aquifer system, and that the time required for gas dissolution was shorter than the time steps used (two to 120 days). The initial methane concentration was assumed to be below saturation in parts of the middle and lower aquifers, such that

$$S_{sg} = 0, \text{ for } (p > p_b) \quad (15)$$

where p_b is the bubble pressure at which the dissolved gas concentration C_w is at saturation, so that gas exsolution did not occur until declining water levels lowered the pressure p in the aquifer below p_b .

Optimum parameter values in model B were estimated with UCODE (Poeter and Hill 1998), a nonlinear regression method similar to MODFLOWP, in which model sensitivity to certain parameters is estimated through a perturbation technique, rather than computed directly from an analytical expression, as in MODFLOWP. The set of estimated parameters was increased from six to eight to include p_b values for the middle and lower aquifers. Estimated specific-storage values for the middle and lower aquifers were near the upper end of the range reported for sand and gravel aquifers ($7.6 \times 10^{-6} \text{ m}^{-1}$) from extensometer data (Table 2). Hydraulic conductivity of the lower aquifer was estimated to be 73 m/d, less than the 91 m/d estimated by model A, in which the specific-storage value was larger and required a larger hydraulic conductivity to simulate the rapid propagation of drawdown through the lower aquifer. The initial methane concentrations corresponding to the estimated p_b values were 170 mg/L in the middle aquifer and 390 mg/L in the lower aquifer.

Including the effects of gas exsolution in model B increased model error by about 20% (Table 2). Predicted drawdowns near the collapse area were larger than those computed with S_s values estimated by the regression (Figure 3a), but matched more closely the observed drawdowns in areas farther away (Figure 3b and 3c).

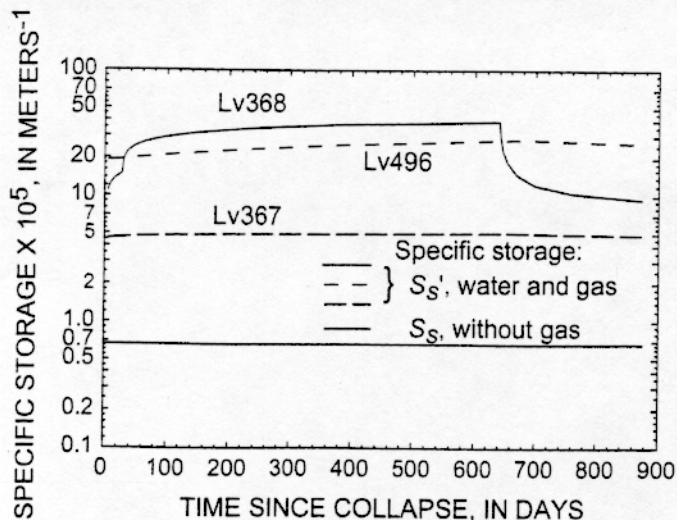


Figure 4. Change in specific storage in model B during water level drawdown and recovery at selected wells screened in lower aquifer in the Genesee Valley, 1994 to 1996.

Model bias decreased when the effects of gas exsolution were included, but the trend of underpredicting drawdowns in wells far from the collapse area remained.

The resulting S_s' values near the point of maximum drawdown at the collapse area ranged from $1.1 \times 10^{-4} \text{ m}^{-1}$ to $4.0 \times 10^{-4} \text{ m}^{-1}$ (well Lv368, Figure 4). The S_s' value was initially greater ($1.9 \times 10^{-4} \text{ m}^{-1}$) at the northern end of the valley (well Lv496, Figure 4), where the pressure is lower than at the collapse area because the lower aquifer is shallower (depths of 65 m and 145 m, respectively). The maximum S_s' value at well Lv496 ($2.8 \times 10^{-4} \text{ m}^{-1}$) was lower than at the collapse area, however, because drawdown was less. Values of S_s' in the south, where the lower aquifer's depth exceeds 215 m, ranged from $4.7 \times 10^{-5} \text{ m}^{-1}$ to $5.2 \times 10^{-5} \text{ m}^{-1}$ (well Lv367, Figure 4). Unlike effective specific storage values near the collapse area, values at the northern and southern ends of the valley remained unchanged after the mine was filled in January 1996 because water levels continued to decline at these locations and did not begin to recover until several months later. The maximum pore volume occupied by gas was calculated to be 4.3% from the release of stored water at the collapse area and less than 1% at the other two locations.

Discussion

Although model A (with a constant specific-storage value) represents the drawdown and recovery of water levels reasonably well, the large values of specific storage estimated through the regression suggest that more water was released from storage than can be accounted for by the compressibility of water and aquifer material alone. Incorporating the exsolution of gas from ground water (model B) allowed the use of realistic specific-storage values to represent water and aquifer compressibility. Model results indicate that the additional release of water through gas exsolution probably lessened water level declines near the collapse area and delayed the propagation of drawdowns into areas away from the collapse.

The gas-venting of wells in 1995 indicates large-scale production of biogenic gas during the period of water level decline that accompanied the flooding of the mine. Methane concentrations in water samples collected in 1999, more than five years after the mine collapse and three years after the mine was completely flooded, suggest that the quantity of biogenic gas has been largely depleted, a

conclusion consistent with the cessation of gas production from all but one of the vented wells. The aquifer system might have been charged with biogenic gas before the mine collapse and lost nearly all of the gas as pressures in the aquifers dropped during mine flooding. If this interpretation is correct, methane concentrations should slowly increase with the continuing production of biogenic gas.

The error in model simulations can be partly explained by uncertainty concerning the initial concentration of gas in ground water, the fate of the exsolved gas, and the effect of gas saturation on the relative permeability of water in the confined aquifer system. If the initial gas concentration was less than estimated, gas would not have exsolved until declining water levels decreased the gas solubility, resulting in specific-storage values smaller than those simulated and water level declines larger than those predicted far from the collapse area. Lower initial methane concentrations in parts of the aquifer system north and south of the collapse area could therefore explain the underprediction of drawdowns in these areas.

The result that simulated recovery of water levels is faster than the observed recovery also suggests that other significant processes are not represented in the model. Some of the exsolved gas migrated upward from the lower aquifer and discharged from the aquifer system, possibly through the collapse area or along the valley walls. Although the rate of gas exsolution was probably rapid because gas was present throughout the aquifer pore volume, the rate of solution was probably slower because gas transfer occurs through the interface separating gas-filled from water-filled pores, and the interfacial area would be smaller once a gas phase developed. A relatively high rate of gas exsolution followed by a lower rate of gas solution could explain the observed rapid drawdown of water levels followed by a relatively slow water level recovery.

If gas occupied 4.3% of the pore volume in the lower aquifer, as calculated in model simulations, the relative permeability of aquifer material to water (K_w) could decrease by about 33% if the gas were distributed uniformly throughout the pore volume (Coats and Richardson 1967; Charbeneau 2000). This condition would probably not persist, however, because the gas would soon migrate upward and form bubbles that would be trapped by the lower confining layer, thereby decreasing the saturated thickness (and transmissivity) by about only 4%. If gas migration were impeded, the decreased K_w could delay water level recovery in some parts of the lower aquifer. Additionally, upward migration of gas along the valley walls could decrease the K_w of permeable sediments that provide hydraulic connection between the confined aquifers and land surface and thereby decrease the potential for recharge and slow the recovery of water levels.

A two-phase flow model that represents water and gas movement could be used to simulate gas migration and its potential effects on relative permeability, but the application of such a model in this setting would be difficult because the initial gas concentration, the migration pathways, and the altitude and topography of the bottom of the lower confining layer, which probably forms a barrier to upward gas migration, are uncertain.

Conclusions

Although specific storage can usually be treated as a constant aquifer property, the presence of dissolved gas in ground water can cause specific storage to increase with decreasing pressure. In a confined aquifer undergoing water level decline, decreasing fluid pressure lowers the gas solubility, allowing gas to exsolve from the water and form a free phase if the dissolved gas concentration exceeds the

gas solubility. A gas-partitioning equation that relates the volume of gas exsolution to the decline in hydraulic head indicates that specific storage is a function of hydraulic head and the dimensionless Henry's law constant for the dissolved gas. Incorporating this relation in a ground water flow model to simulate discharge from a confined aquifer system to a collapsed salt mine allowed the use of representative compressibility values for water and aquifer material. Model results suggested that methane exsolution greatly increased the effective specific storage of the aquifer system and significantly diminished water level declines. The initial concentration of methane in ground water is uncertain, however, and a two-phase flow model representing both water and gas movement would be needed to simulate gas migration and its potential effects on relative permeability of the aquifer material. Similar effects could occur with other dissolved gases such as carbon dioxide and hydrogen sulfide if they are present at high concentrations; however, concentrations of these constituents are typically low and the effect would probably be minor.

Editor's Note: The use of brand names in peer-reviewed papers is for identification purposes only and does not constitute endorsement by the authors, their employers, or the National Ground Water Association.

Acknowledgments

Paul Hseih and Chris Neuzil of the U.S. Geological Survey provided contributions to the theoretical derivations presented in this paper. Several anonymous reviewers provided helpful comments and suggestions that improved the manuscript.

References

- Adrian, N.R., J.A. Robinson, and J.M. Suflita. 1994. Spatial variability in biodegradation rates as evidenced by methane production from an aquifer. *Applied and Environmental Microbiology* 60, no. 10: 3632-3639.
- Barker, J.F., and P. Fritz. 1981. The occurrence and origin of methane in some groundwater flow systems. *Canadian Journal of Earth Science* 18, 1802-1816.
- Bear, Jacob. 1979. *Hydraulics of Groundwater*. New York: McGraw-Hill Book Co.
- Bredehoeft, J.D. 1967. Response of well-aquifer systems to earth tides. *Journal of Geophysical Research* 72, no. 12: 3075-3087.
- Charbeneau, R. 2000. *Groundwater Hydraulics and Pollutant Transport*. Upper Saddle River, New Jersey: Prentice Hall.
- Coats, K.H., and J.G. Richardson. 1967. Calculation of water displacement by gas in development of aquifer storage. *Society of Petroleum Engineers Journal*, no. 2: 105-112.
- Faber, E., and W. Stahl. 1984. Geochemical surface exploration for hydrocarbons in the North Sea. *American Association of Petroleum Geologists Bulletin* 68, 363-386.
- Hall, R. 1996. Interview by author, July 12, Dansville, New York.
- Heywood, C.E. 1998. Piezometric-extensometric estimations of specific storage in the Albuquerque Basin, New Mexico. In *Land Subsidence Case Studies and Current Research. Proceedings of the Dr. Joseph F. Poland Symposium*, ed. J.W. Borchers, 435-440. Belmont, California: Star Publishing Co.
- Hill, M.C. 1992. A computer program (MODFLOWP) for estimating parameters of a transient, three-dimensional ground-water flow model using nonlinear regression. U.S. Geological Survey Open-File Report 91-484.
- James, A.T. 1983. Correlation of natural gas by use of carbon isotopic distribution between hydrocarbon components. *American Association of Petroleum Geologists Bulletin*, 67, 1176-1191.
- Jarso, J., and G. Destouni. 2000. Degassing of deep groundwater in fractured rock around boreholes and drifts. *Water Resources Research* 36, no. 9: 2477-2492.
- Jenden, P.D., D.J. Drazan, and I.R. Kaplan. 1993. Mixing of thermogenic natural gases in Northern Appalachian Basin. *American Association of Petroleum Geologists Bulletin* 77, 980-998.
- Jones, V.T., and R.J. Drozd. 1983. Predictions of oil or gas potential by near surface geochemistry. *American Association of Petroleum Geologists Bulletin* 67, 932-952.
- Kammerer, J.C., and W.A. Hobba. 1967. The geology and availability of ground water in the Genesee River basin, New York and Pennsylvania; Appendix I, Ground-water resources of the Genesee River basin. Albany, New York: New York State Water Resources Commission.
- King, G.M., and W.J. Wiebe. 1978. Methane release from soils of a Georgia salt marsh. *Geochimica et Cosmochimica Acta* 42, 343-348.
- Leake, S.A. 1991. Documentation of a computer program to simulate aquifer-system compaction using the modular finite-difference ground-water flow model. *U.S. Geological Survey Techniques of Water-Resources Investigations*, Book 6, Chapter A2.
- Li, Y.-K., and L.X. Nghiem. 1986. Phase equilibria of oil, gas and water/brine mixtures from a cubic equation of state and Henry's law. *Canadian Journal of Chemical Engineering* 64, 486-496.
- Martini, A.M., J.M. Budai, L.M. Walter, and M. Schoell. 1996. Microbial generation of economic accumulations of methane within a shallow organic-rich shale. *Nature* 383, 155-157.
- McAuliffe C. 1966 Solubility in water of paraffins, cycloparaffins, olefin, acetylene, cycloolefin and aromatic hydrocarbons. *Journal of Physical Chemistry* 70, 1267-1275.
- Milliken, L.D. 1995. Written communication by author, April 26, Clarks Summit, Pennsylvania.
- Milliken, L.D. 1996. Interview by author, August 8, Clarks Summit, Pe Pennsylvania.
- Nelson, G.L. 1982. Vertical movement of ground water under the Merrill field land fill, Anchorage, Alaska. U.S. Geological Survey Open-File Report 82-1016.
- Parkin, T.B., and W.W. Simpkins. 1995. Contemporary groundwater methane production from Pleistocene carbon. *Journal of Environmental Quality* 24, 367-372.
- Poeter, E.P., and M.C. Hill. 1998. Documentation of UCODE, a computer code for universal inverse modeling. U.S. Geological Survey Water-Resources Investigations Report 98-4080.
- Riley, F.S. 1969. Analysis of borehole extensometer data from central California. In *Land Subsidence*, ed. L.J. Tison, 423-431. International Association of Hydrologists Publication 89.
- Riley, F.S. 1998. Mechanics of aquifer systems—The scientific legacy of Joseph F. Poland. In *Land Subsidence, Case Histories and Current Research, Proceedings of the Dr. Joseph F. Poland Symposium on Land Subsidence*, ed. J.W. Borchers, 13-37. Belmont, California: Star Publishing Co., Association of Engineering Geologist Special Publication no. 8.
- Romanowicz, E.A., J.P. Chanton, and P.H. Glaser. 1995. Temporal variations in dissolved methane deep in the Lake Agassiz Peatlands, Minnesota. *Global Biogeochemical Cycles* 9, 197-212.
- Schwarzenbach, P.M., P.M. Gschwend, and D.M. Imboden. 1993. *Environmental Organic Chemistry*. New York: John Wiley and Sons.
- Song K.Y., G. Feneyrou, F. Fleyfel, R. Martin, J. Lievois, and R. Kobayashi. 1997. Solubility measurements of methane and ethane in water at and near hydrate conditions. *Fluid Phase Equilibria* 128, 249-260.
- Stahl, W., E. Faber, B.D. Carey, and D.L. Kirksey. 1981. Near-surface evidence of migration of natural gas from deep reservoirs and source rocks. *American Association of Petroleum Geologists Bulletin* 65, 1543-1550.
- Wang, P., E.H. Stenby, G.A. Pope, and K. Sepehrnoori. 1996. Simulation of flow behavior of gas condensate at low interfacial tension. *In Situ* 20, no. 2: 199-219.
- Whiticar, M.J., E. Faber, and M. Schoell. 1986. Biogenic methane formation in marine and freshwater environments: CO₂ reduction vs. acetate fermentation-isotope evidence. *Geochimica et Cosmochimica Acta* 50, 693-709.
- Yager, R.M., T.S. Miller, and W.M. Kappel. 2001. Simulated effects of a 1994 salt-mine collapse on ground-water flow and land subsidence in a glacial aquifer system, Livingston County, New York. U.S. Geological Survey Professional Paper 1629.